Singular perturbation theory for phase-front dynamics and pattern selection



1990 J. Phys. A: Math. Gen. 23 L803

(http://iopscience.iop.org/0305-4470/23/16/005)

J. Phys. A: Math. Gen. **23** (1990) L803-L808. Printed in the UK

LETTER TO THE EDITOR

# Singular perturbation theory for phase-front dynamics and pattern selection

K R Elder and Martin Grant

Centre for the Physics of Materials and Department of Physics, McGill University, Rutherford Building, 3600 University Street, Montréal, Québec, H3A 2T8 Canada

Received 13 June 1990

**Abstract.** A class of phase-front dynamics equations is investigated through a particular singular perturbative expansion in a late-time, restricted-wavelength limit. The approximate solution provides a detailed description of the dynamics of pattern formation in all dimensions and reproduces some aspects of marginal stability theory in one dimension. A universal form for the dynamic structure factor is obtained for non-conserved systems. The results are applied to a model of the onset of the Rayleigh-Benard instability, the Swift-Hohenberg equation.

There exist a wide range of natural phenomena that involve the growth of multiphase spatial patterns from initially unstable states. Examples of such processes include the kinetics of domain growth in first-order transitions [1, 2], the onset of Rayleigh-Benard convection [3-6], the twist Freedericksz transition in nematic crystals [7], phase separation in block copolymer systems [8] and population dynamics [9]. To study these systems, simple continuum dynamical models have been introduced to describe the dynamics of the slow modes of growth that display spatial variations. Often these models are realized in terms of nonlinear partial differential equations. Well known examples, in the field of phase-front dynamics, include the Swift-Hohenberg equation [3], the extended Fisher-Kolomogorov equation [10], the block copolymer equation [8], the time-dependent Ginzburg-Landau equation [2, 11] and the Fisher equation [9]. The difficulty in analysing these equations lies in a subtle coupling between nonlinearities and spatial gradients. For this reason, analytical results are often restricted to systems which display spatial gradients in only one dimension (which can be probed in some experimental systems).

In this letter, a technique, developed to study the growth of fluctuations in lasers by Suzuki [1] and in order-disorder transitions by Kawasaki *et al* [2] (and more recently in population dynamics [12] and uni-axial ferromagnetic films [3]), is generalized to a class of phase dynamics problems. Some results for one dimension are obtained, but the main value of this treatment is the predictions for pattern formation in dimension $d = 2$ and 3. The results indicate a connection between the diverse range of physical processes mentioned above due to the dominance of a single Fourier wavenumber in the late stages of growth. In summary a singular perturbative expansion is employed in which the most dangerous diagrams are resummed in a particular asymptotic approximation discussed below. The analysis disentangles the subtle coupling between nonlinearities and spatial gradients through a nonlinear transformation at late times. The results of this calculation provide the complete, although approximate,

0305-4470/90/160803+06$03.50  

probability distribution function in all dimensions, in the absence of thermal noise. In one-dimensional front propagation problems, some aspects of the marginal stability theory [4, 10, 14] for the phase front are found to be a direct consequence of the approach. In higher dimensions an explicit universal form of the dynamic structure factor is given which can be tested numerically or experimentally.

The general equation considered is

$$\frac{\partial\psi(\boldsymbol{r}, t)}{\partial t} = \alpha(\nabla^2)\psi(\boldsymbol{r}, t) - \beta(\nabla^2)\psi(\boldsymbol{r}, t)^n \tag{1}$$

where $\psi$ is the field that displays spatial variation, $n$ is an integer larger than one, $t$ is time, $\boldsymbol{r}$ is a spatial coordinate, and $\alpha$ and $\beta$ are functions of $\nabla^2$. In Fourier space, $\alpha(k)$, where $k$ is the wavenumber, contains one positive maximum at $k_m$, and $\beta$ must be a positive constant, except for $d = 1$, as discussed below. When $n$ is odd, (1) contains two stable states, while when $n$ is even there exists only one stable state. Equation (1) encompasses many models, including those mentioned above.

An outline of the approximation scheme follows [15]. The first step is to formally expand (1) in terms of the bare propagator $\psi^0(\boldsymbol{k}, t) = e^{\alpha(k)t}\psi(\boldsymbol{k}, 0)$, as shown in figure 1. A straight line depicts that propagator, while a line terminating in a square represents the nonlinear perturbation $\sim -\beta(k)\int_0^t dt_1\, e^{\alpha(k)(t-t_1)}\int d\boldsymbol{k}_1\int d\boldsymbol{k}_2 \ldots \int d\boldsymbol{k}_n\, \delta(\boldsymbol{k} - \Sigma_{i=1}^n \boldsymbol{k}_i)$. The diagrammatic structure indicates that the $b$th-order diagram, where $b$ is the number of vertices, is proportional to $\psi^0(\boldsymbol{r}, t)^{b(n-1)+1}$. Since $\psi^0(\boldsymbol{r}, t)$ grows exponentially with time, every term in the expansion is required to obtain a solution at late times. Thus, ordering the diagrams by the vertices gives a singular perturbation expansion.

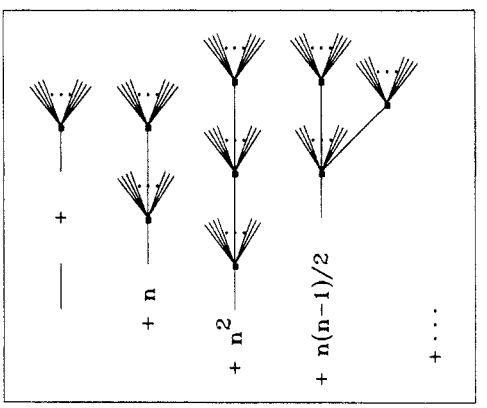


**Figure 1.** Diagrammatic expansion of (1). A straight line represents the bare propagator and the lines terminating in a square corresponds to the nonlinear interaction.

To resum the infinite singular perturbation series, we consider the most dangerous diagrams (or more precisely the most dangerous parts of each diagram) in a particular asymptotic limit. The two approximations restrict the results to the late-time regime and to systems where the interface structure and detailed shape is unimportant. The $b$th-order diagram contains $b$ integrals over time which are approximated by assuming that the largest pole (in Laplace space) provides the dominant contribution to the $b$th-order diagram. The error due to this approximation (i.e. $(t^{d/2} e^{-\alpha(k_m^2)t})^{n-1}$) is asymptotically small. The second approximation (Laplace's integral approximation

[16]) implies that the dominant contribution to the $b$th-order diagram occurs when $|\boldsymbol{k}_i| = |\boldsymbol{k} - \sum_{i=1}^{b(n-1)} \boldsymbol{k}_i| = k_m$ (where, $\boldsymbol{k}_i$ is an integration variable), for $|\boldsymbol{k}| \approx k_m$. Roughly speaking, this amounts to assuming that the late stage dynamics are dominated by minimizing the Lyapunov functional† (or free energy functional) that corresponds to (1). Although these are late-time approximations, and consequently provide an asymptotic solution to $\psi(\boldsymbol{r}, t)$, the solution will be valid at early times if the fluctuations of the initial state are small (i.e. if $\psi(\boldsymbol{r}, t=0)$ is small).

On obtaining the approximate form of the $b$th-order diagram and its multiplicity, the series is resummed following Kawasaki *et al* [2]. The solution for the distribution function is

$$P(\{\psi\}, t) \approx N \exp\left(\frac{-n}{n-1} \int \frac{\mathrm{d}\boldsymbol{r}}{v_0} \ln(1-(\psi(\boldsymbol{r})/A)^{n-1})\right) \times P_0\left(\mathrm{e}^{-\alpha(\nabla^2)t} \frac{\psi(\boldsymbol{r})}{(1-(\psi(\boldsymbol{r})/A)^{n-1})^{1/(n-1)}}\right) \tag{2}$$

where, $A \equiv (\alpha(k_m)/\beta(k_m))^{1/(n-1)}$, $P_0$ is the initial distribution function, $N$ is a normalization constant, and $v_0$ is the coarse graining cell volume. This is the main result of this letter. The equivalent representation in order parameter space is

$$\psi(\boldsymbol{r}, t) \approx \frac{\psi^0(\boldsymbol{r}, t)}{(1+(\psi^0(\boldsymbol{r}, t)/A)^{n-1})^{1/(n-1)}}. \tag{3}$$

Equation (3) shows that the interface positions (or nodes in the pattern) $\boldsymbol{r}_1$ are described by $\psi^0(\boldsymbol{r}_1, t) = 0$ and the magnitude of the bulk fluctuations is $A$. Thus, (3) gives a simple description of the dynamical behaviour of the interface position for the class of problems considered. The main deficiency is that at late times (3) predicts an infinitely sharp transition from one phase to the other, unlike the stationary solution of (1) which predicts a more general transition.

In one-dimensional front-propagation problems, one often considers the dynamics of a stable phase moving into an unstable one. A central problem addressed by the marginal stability hypothesis [4, 10, 13] is to determine how the velocity of the front and a particular wavenumber of the pattern formed by the front is selected. In our treatment, it can be shown that the velocity and wavenumber chosen at the front is indeed the same as that predicted by marginal stability, even though the wavenumber in the bulk phase is unfortunately fixed as $k_m$. For simplicity the initial state is chosen to be $\psi(x, 0) = \delta(x)$. Using the saddle-point approximation [17] to evaluate $\psi^0(x, t)$ and (3) to evaluate $\psi(x, t)$ we obtain,

$$v = \frac{\mathrm{Re}(\alpha(k^*))}{\mathrm{Im}(k^*)} + \frac{\ln(|Ch''(k^*)|t/2\pi)}{2t\,\mathrm{Im}(k^*)} \tag{4}$$

$$\lambda = 2\pi v \left(\mathrm{Im}(h(k^*)) + \frac{\pi - \arg[h''(k^*)]}{2t}\right)^{-1} \tag{5}$$

† For constant $\beta$ the Lyapunov functional ($F$) associated with (1) is

$$F = -\int \mathrm{d}\boldsymbol{r}\left[\tfrac{1}{2}\int \mathrm{d}\boldsymbol{r}_1\, \alpha(\nabla^2)\psi(\boldsymbol{r})\psi(\boldsymbol{r}_1)\delta(\boldsymbol{r}-\boldsymbol{r}_1) - \frac{\beta}{n+1}\psi^{n+1}(\boldsymbol{r})\right].$$

To be precise the diagrams are maximized at $k = k_m$, which minimizes $F$ in the absence of mode coupling. For one-dimensional patterns it is known [6] that mode coupling can cause a different $k$ to minimize $F$.

(note that the right-hand side of (4) and (5) also depends on $v$). In (4) and (5), $v$ ($\equiv x/t$) is the velocity of the front, $\lambda$ is the wavelength of the front, $A$ is the amplitude of the fluctuations, $C$ is a constant and $k^*$ is defined by

$$\mathrm{Re}\left(\frac{\partial h(k)}{\partial k}\bigg|_{k^*}\right) = \mathrm{Im}\left(\frac{\partial h(k)}{\partial k}\bigg|_{k^*}\right) = 0 \tag{6}$$

where, $h(k) = \mathrm{i}kv + \alpha(k)$. These results are identical to the marginal stability predictions in the asymptotic time regime. This is because the basic premise of that theory is that the linear solution describes the phase front. Similarly, (3) reduces to the linear solution at the phase front for all times. The extra terms in the equation for the front velocity and wavelength do not appear in the marginal stability theory since they are early-time corrections to the saddle point approximation of the linear solution. An important deficiency of the present approach, however, is that the correct wavenumber in the bulk usually differs from $k_m$ in $d = 1$, since the wavelength selected by the front (i.e. $\lambda$) does not minimize the free energy functional. In higher dimensions interface curvature provides a mechanism to dislodge the system from any marginal stable solutions.

To illustrate the $d = 1$ results, consider the Swift-Hohenberg equation, which is defined by $\alpha(k) = \gamma^2 - (k^2 - 1)^2$ and $\beta = 1$, where $\gamma$ is a control parameter. A comparison of a numerical solution with (3) for an initial state of $\psi(x, 0) = 0.1\,\mathrm{e}^{-x}$ is given in figure 2 for $\gamma = 0.9$. Figure 2($a$) shows the approximate solution presented in this work accurately describes the early stages of growth. In the latter stages of growth (figures

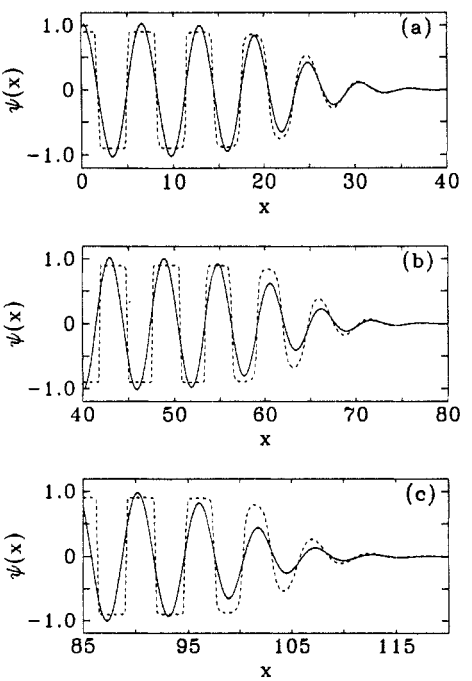


**Figure 2.** Comparison of numerical and analytic solution of the one-dimensional Swift-Hohenberg equation. The numerical solution is the full curve and the broken curve is from (3). In this figure, $\mathrm{d}x = 0.25$, $\gamma = 0.9$ and $\psi(x, t = 0) = 0.1\,\mathrm{e}^{-x}$. Figures 2($a$), 2($b$) and 2($c$) respectively correspond to $t = 10$, 20 and 30.

2(*b*) and 2(*c*)), discrepancies in the bulk begin to appear. This is because for $\gamma = 0.9$, $2\pi/\lambda = 1.076$ while $k_m = 1$, in the asymptotic time regime. Nevertheless, the leading phase front is described correctly.

In higher dimensions, a quantity of importance is the dynamic structure factor ($S(k, t) = \langle|\psi(\boldsymbol{k}, t)|^2\rangle$, where the angular brackets denote an average over the initial state) since it can be measured experimentally by many methods. It is straightforward to calculate $S(\boldsymbol{k}, t)$ from (2) for a system that is Gaussian correlated at $t = 0$. In real space, the result is

$$S(\boldsymbol{r}, t) = A^2 \int_0^\infty \mathrm{d}w\, \mathrm{e}^{-w} \int_0^{2\pi} \frac{\mathrm{d}\phi}{2\pi} \frac{z^+ z^-}{[(1+(z^+)^{n-1})(1+(z^-)^{n-1})]^{1/(n-1)}} \tag{7}$$

where , $z^\pm \equiv \sqrt{2wS^0(0, t)}\,\sin(\phi \pm \theta/2)/A$, $\theta \equiv \cos^{-1}(S^0(\boldsymbol{r}, t)/S^0(0, t))$ and $S^0(\boldsymbol{r}, t)$ is the linear structure factor (i.e. $\mathrm{e}^{2\alpha(\nabla^2)t}S(r, 0)$). At late times $S^0(0, t)$ becomes large and (7) can be approximated in the particularly simple form (for $n$ odd†),

$$S(\boldsymbol{r}, t) = f(S^0(\boldsymbol{r}, t)/S^0(0, t)). \tag{8}$$

The universal function $f(x) \equiv (2A^2/\pi)\sin^{-1}(x)$, has been obtained previously for the particular case of the kinetics of the order-disorder transition [2]. It would be of interest to experimentally or numerically investigate the universal nature of the structure factor we predict. In the large-wavenumber limit, (8) is consistent with Porod's law [18], $S(k, t) \approx 1/k^{d+1}$. This is a geometric consequence of sharp interfaces. The one-point distribution for an initial Gaussian distribution is

$$\rho(\psi, t) = \frac{(2\pi S^0(0, t))^{-1/2}}{(1-(\psi/A)^{n-1})^{n/(n-1)}} \exp\left(\frac{-\psi^2}{2S^0(0, t)(1-(\psi/A)^{n-1})^{2/(n-1)}}\right). \tag{9}$$

The structure of (9) indicates that an initially single-peaked function evolves into a bimodal distribution. At infinite time, this distribution is zero everywhere except at $\psi = \pm A$, which corresponds to sharp domain walls.

For the two-dimensional Swift-Hohenberg equation, $S(k, t)$ as determined from (7) is shown in figure 3. This function develops a peak at $k = 1$, as highly interconnected domains of width $2\pi$ dynamically evolve from the random initial state. The one-point distribution for the Swift-Hohenberg equation is presented in the inset of figure 3.

To conclude, the technique presented in this letter provides an analytic description of domain growth and front propagation is non-conserved systems and characterizes phase-front propagation in one-dimensional systems. The approximate analytic description also provides a universal form of the dynamical structure factor that can be experimentally or numerically investigated. In the future we intend to extend this technique to include conserved systems, where interface curvature plays an important role.

This work was supported by the Natural Sciences and Engineering Research Council of Canada, les Fonds pour la Formation de Chercheurs et l'Aide a la Recherche de la Province du Quebec and by a NATO Collaborative Research Grant project number CRG 890482. We thank Jorge Viñals, Maxi San Miguel, Emilio Hernández-García, Chris Roland, and Rashmi Desai for useful discussions.

† When $n$ is even the system has only one stable state, and thus $S(\boldsymbol{r}, t \to \infty) \to A^2$.

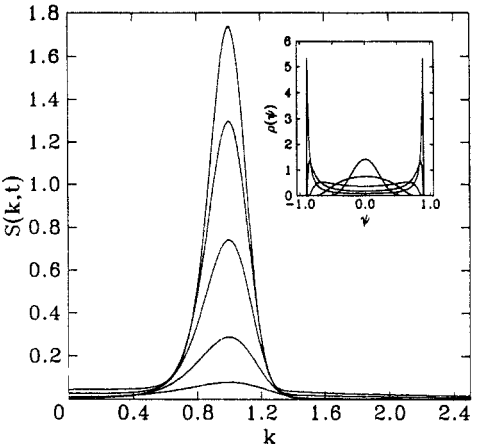


**Figure 3.** The time dependence of the $S(k, t)$ is displayed for $\gamma = 0.9$ as calculated from (7) for the Swift-Hohenberg equation. From bottom to top the lines correspond to $t = 1$, 2, 3, 4 and 5. In the inset the one-point distribution function is shown for the same times as given above. $t = 1$ corresponds to the line that peaks at $\psi = 0$ and $t = 5$ corresponds to the line with the two highest peaks.

## References


[1] Suzuki M 1976 *Prog. Theor. Phys.* **56** 77
Suzuki M 1976 *Prog. Theor. Phys.* **56** 477
Suzuki M 1977 *J. Stat. Phys.* **16** 11
[2] Kawasaki K, Yalabik M C and Gunton J D 1978 *Phys. Rev.* A **17** 455
Ohta T, Jasnow D and Kawasaki K 1982 *Phys. Rev. Lett.* **49** 1223
[3] Swift J and Hohenberg P C 1977 *Phys. Rev.* A **15** 319
[4] Dee G and Langer J S 1983 *Phys. Rev. Lett.* **50** 383
[5] Steinberg V, Ahlers G and Cannell D S 1985 *Phys. Scr.* **T9** 111
[6] Pomeau Y and Manneville P 1979 *J. Physique Lett.* **40** L609
[7] Lonberg F, Fraden S S, Hurd A J and Meyer R E 1984 *Phys. Rev. Lett.* **52** 1903
Hui Y W, Kuzma M R, San Miguel M and Labes M M 1985 *J. Chem. Phys.* **83** 288
San Miguel M and Sagues F 1987 *Phys. Rev.* A **36** 1883
[8] Oono Y and Shiwa Y 1987 *Mod. Phys. Lett.* **B1** 49
Liu F and Goldenfeld N 1989 *Phys. Rev.* A **39** 4805
[9] Fisher R A 1937 *Ann. Eugenics* **7** 355
[10] Dee G T and van Saarloos W 1988 *Phys. Rev. Lett.* **60** 2641
[11] Mazenko G F, Valls O T and Ruggiero P 1989 *Phys. Rev.* B **40** 384
[12] Puri S, Elder K and Desai R C 1990 *Phys. Lett.* A to be published
[13] Roland C and Desai R C 1990 *Preprint*
[14] van Saarloos W 1987 *Phys. Rev. Lett.* **58** 2571
van Saarloos W 1988 *Phys. Rev.* A **37** 211
[15] Elder K R and Grant M 1990 in preparation
[16] Bender C M and Orszag S A 1978 *Advanced Mathematical Methods for Scientists and Engineers* (New York: McGraw-Hill)
[17] De Bruijn N G 1961 *Asymptotic Methods in Analysis* (Amsterdam: North-Holland)
[18] Porod G 1982 *Small Angle X-ray Scattering* ed O Glatter and O Kratsky (New York: Academic)